

Modeling of equiaxed and columnar dendritic growth of magnesium alloy

WU Meng-wu^{1,2}, XIONG Shou-mei^{1,2}

1. Department of Mechanical Engineering, Tsinghua University, Beijing 100084, China;
2. State Key Laboratory of Automobile Safety and Energy, Tsinghua University, Beijing 100084, China

Received 7 September 2011; accepted 20 February 2012

Abstract: Based on the cellular automaton (CA) method, a numerical model was developed to simulate the dendritic growth of magnesium alloy with HCP crystal structure. The growth kinetics was calculated from the complete solution of the transport equations. By defining a special neighborhood configuration with the square CA cell, and using a set of capturing rules which were proposed by BELTRAN-SANCHEZ and STEFANESCU for the dendritic growth of cubic crystal metals during solidification, modeling of dendritic growth of magnesium alloy with different growth orientations was achieved. Simulation of equiaxed dendritic growth and columnar dendritic growth under directional solidification was carried out, and validation was performed by comparing the simulated results with the experimental results and those in the previously published works.

Key words: magnesium alloy; dendritic growth; cellular automaton method; growth orientation

1 Introduction

The development of extraction and manufacturing technologies of magnesium alloy has promoted its worldwide use, making it the third most commonly used structural metal. Especially in transportation industry, the application of magnesium alloy parts particularly caters for the demand of weight reduction, which seems to be the best cost-effective option for significant decreasing of fuel consumption and CO₂ emission [1–3].

The performance of castings of magnesium alloy is strongly influenced by the as-cast microstructure formed during solidification, such as, the grain size, secondary arm spacing, and micro-segregation. Accordingly, the key aspect of casting technology is to investigate the effect of process parameters on the microstructure of magnesium alloy, consequently, optimize the process parameters and control the microstructure during the casting process. Among the methods of study, numerical modeling and simulation has been widely used as a powerful tool for simulating and predicting the time-dependent microstructure evolution during various solidification processes. In the last two decades, extensive efforts have been dedicated to develop numerical methods suitable for the microstructure simulation. Among those deterministic and stochastic

methods, the cellular automaton (CA) method has been used extensively to predict a wide range of realistic phenomena associated with dendritic or nondendritic microstructure formation [4–8]. It has the attractive advantages such as simplicity of formulation and computational convenience when implemented to solve phase transition problems with an acceptable computational efficiency. However, an artificial anisotropy is introduced with the use of CA cells and the corresponding neighborhood configuration and capturing rules. This artificial anisotropy becomes significant when the preferential growth direction is not aligned with the axis of the cell. Most of the published works using the CA method focus on the microstructure simulation of cubic crystal metals, while the CA method has many difficulties in simulating the microstructure of magnesium alloy with HCP crystal structure.

In the present paper, a cellular automaton model was proposed to simulate the dendritic growth of magnesium alloy. As verified in case studies, modeling of dendritic growth with six-fold symmetry and different growth orientations was achieved. The model was applied to simulate the equiaxed dendritic growth and columnar dendritic growth under directional solidification, and the effects of certain factors on the dendritic growth, including the cooling rate and the temperature gradient, etc, were discussed then.

2 Model description

2.1 Type of CA cell and neighborhood configuration

The CA method is a set of algorithms used to describe the evolution of discrete systems in time and space. For the microstructure simulation, a CA model consists of: 1) the geometry of a cell, 2) the state of a cell, 3) the neighborhood configuration, and 4) the transition rules that determine the state of a given cell during one time step. Generally, the most commonly used cell shapes are square and cubic, respectively in two and three dimensional coordinates. As mentioned above, most of the published works using the CA method focus on the microstructure simulation of cubic crystal metals. In the early stages of model development, the artificial anisotropy introduced with the use of square cells or cubic cells was desirable, since it reproduced the crystallographic preferential growth directions of cubic crystal metals. Unfortunately, this artificial anisotropy becomes a liability when the preferential growth directions are not aligned with the axis of the cell. Therefore, modeling of dendritic growth with different growth orientations is particularly difficult. All the simulated dendrites are forced to grow in alignment with the cell axis regardless of the initial orientations.

As for the commonly available magnesium alloys, such as AZ91 and AM50, it seems that the CA model with the use of square cells (the present work focuses on modeling and simulating in two dimensional coordinates) is not capable of modeling the dendritic morphology with six-fold symmetry, the schematic diagram of which is illustrated in Fig. 1. Accordingly, HUO et al [9] and YIN et al [10] adopted hexagonal cells in the CA model, and by this means, simulation of the dendritic growth of magnesium alloy was achieved. However, the use of hexagonal cells brings some difficulties in the calculation of the solute field and growth kinetics, etc. Moreover, the dendritic growth orientation is limited to the cell axis and different orientations are not possible. In the present CA

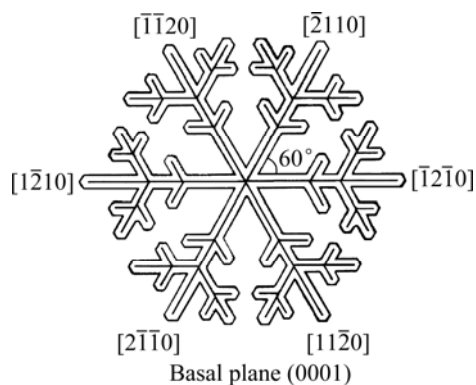


Fig. 1 Sketch of dendritic morphology of magnesium alloy with six-fold symmetry

model, square cells were still used to simulate the dendritic growth of magnesium alloy. Based on the authors' previous work [11], a special neighborhood configuration was defined as shown in Fig. 2. By improving the calculation method of the growth kinetics and defining a set of capturing rules, the present CA model has the capability to simulate the dendritic growth with six-fold symmetry and different growth orientations. More details are available in the following sections.

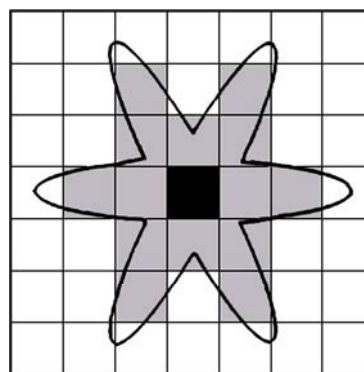


Fig. 2 Definition of neighborhood configuration [11]

2.2 Solute redistribution

During solidification of magnesium alloy, the solute diffusion plays an important role in determining the grain growth morphology and the corresponding microstructure characteristics. In the present work, the magnesium alloy was treated as a binary alloy for simplification. As the solidification proceeds, the solute accumulates at the solidification front due to the solute rejection associated with the solidification of α -Mg. For the calculation of solute field, local equilibrium at the solid/liquid interface was assumed, which can be expressed as:

$$C_S^* = kC_L^* \quad (1)$$

where k is the solute partition coefficient, C_S^* and C_L^* are the equilibrium solute concentrations of the solid and liquid phases at the interface, respectively. Meanwhile, the effect of convection on the solute field was not taken into account. Therefore, the solute redistribution in the liquid and solid can be governed by:

$$\frac{\partial C_L}{\partial t} = \frac{\partial}{\partial x} \left[D_L \frac{\partial C_L}{\partial x} \right] + \frac{\partial}{\partial y} \left[D_L \frac{\partial C_L}{\partial y} \right] + C_L(1-k) \frac{\partial f_s}{\partial t} \quad (2)$$

$$\frac{\partial C_S}{\partial t} = \frac{\partial}{\partial x} \left[D_S \frac{\partial C_S}{\partial x} \right] + \frac{\partial}{\partial y} \left[D_S \frac{\partial C_S}{\partial y} \right] \quad (3)$$

where t is the time; C_L and C_S are the solute concentrations of the liquid and solid, respectively; D_L and D_S are the liquid and solid solute diffusion coefficients; and f_s is the solid fraction. The last term on the right hand side of Eq. (2) represents the solute rejection at the solid/liquid interface due to the increment

of the solid fraction of α -Mg. Since the solutal diffusivity is usually several orders of magnitude smaller than the thermal diffusivity, a zero-flux boundary condition was set to solve the above equations with an explicit finite difference scheme.

2.3 Growth kinetics and orientation

As mentioned above, local equilibrium at the solid/liquid interface was assumed. The equilibrium solute concentration of the liquid at the interface, C_L^* , can be calculated as:

$$C_L^* = C_0 + \frac{T^* - T_L^{eq} + \Gamma K f(\varphi, \theta)}{m_L} \quad (4)$$

where C_0 is the initial solute concentration of the liquid; T^* and T_L^{eq} are the interface and equilibrium liquidus temperatures, respectively; m_L is the liquidus slope; Γ is the Gibbs-Thomson coefficient; K is the curvature of the interface; and $f(\varphi, \theta)$ is the anisotropy function. For the calculation of the interface curvature, K , since the counting method proposed by SASIKUMAR and SREENIVASAN [12] suffers from a deviation of the curvature evaluation significantly depending on the number of cells considered and the cell size, it is calculated based on the physical concept as follows [6]:

$$K = \frac{1}{\left[\left(\frac{\partial f_s}{\partial x} \right)^2 + \left(\frac{\partial f_s}{\partial y} \right)^2 \right]^{3/2}} \cdot \left[2 \frac{\partial f_s}{\partial x} \frac{\partial f_s}{\partial y} \frac{\partial^2 f_s}{\partial x \partial y} - \left(\frac{\partial f_s}{\partial x} \right)^2 \frac{\partial^2 f_s}{\partial y^2} - \frac{\partial^2 f_s}{\partial x^2} \left(\frac{\partial f_s}{\partial y} \right)^2 \right] \quad (5)$$

In order to describe the anisotropy of the surface tension of magnesium alloy, the anisotropy function, $f(\varphi, \theta)$, is given by:

$$f(\varphi, \theta) = 1 + \delta \cos[6(\varphi - \theta)] \quad (6)$$

$$\varphi = \arccos \left(\frac{\partial f_s / \partial x}{\sqrt{(\partial f_s / \partial x)^2 + (\partial f_s / \partial y)^2}} \right) \quad (7)$$

where δ is the anisotropy coefficient, whose value was chosen to be 0.04 in the present work; θ and φ are the angles of the preferential growth direction and the normal to the interface with respect to the x coordinate, respectively.

According to the assumption of solute conservation at the moving solid/liquid interface, the growth velocity of the interface, v_n , can be expressed as:

$$v_n C_L^* (1-k) = \left[-D_L \left(\frac{\partial C_L}{\partial x} + \frac{\partial C_L}{\partial y} \right) + D_S \left(\frac{\partial C_S}{\partial x} + \frac{\partial C_S}{\partial y} \right) \right] \cdot n \quad (8)$$

$$v_n = \frac{1}{C_L^* (1-k)} \left[-D_L \left(\frac{\partial C_L}{\partial x} \cos \varphi + \frac{\partial C_L}{\partial y} \sin \varphi \right) + D_S \left(\frac{\partial C_S}{\partial x} \cos \varphi + \frac{\partial C_S}{\partial y} \sin \varphi \right) \right] \quad (9)$$

Based on the advance of the interface front along the normal to the interface with the normal velocity, the increment of the solid fraction of an interface cell can be calculated as:

$$\delta f_s = \frac{v_n \delta t}{l} \quad (10)$$

$$l = \frac{\Delta s}{\max(|\cos \varphi|, |\sin \varphi|)} \quad (11)$$

where δf_s is the increment of the solid fraction during the time step δt , l is the length of the line along the normal to the interface and passing through the cell center, and Δs is the cell size. The time step, δt , is determined by the solute diffusion coefficient and the growth velocity of the interface, which can be expressed as:

$$\delta t = \frac{1}{5} \min \left(\frac{l}{v_{\max}}, \frac{\Delta s}{D_L}, \frac{\Delta s}{D_S} \right) \quad (12)$$

where v_{\max} is the maximum growth velocity of the interface at the previous time step. When the solid fraction, f_s , of the interface cell becomes greater than unity, the cell changes into a solid cell, and then capturing of the neighboring liquid cells into new interface cells begins.

To the best of our knowledge, only two methods, the decentered square growth technique [5,13] and the virtual interface tracking method [14,15] were reported in the literatures, which can be successfully used to simulate the dendritic growth of cubic crystal metals with arbitrary growth orientations. However, simulation of the dendritic growth of magnesium alloy with different growth orientations has not been reported yet. In the present CA model, using a set of capturing rules which were proposed by BELTRAN-SANCHEZ and STEFANESCU [14] for the dendritic growth of cubic crystal metals during solidification, modeling of the dendritic growth of magnesium alloy with different growth orientations was achieved. More details relating the capturing rules could be found in Refs. [16,17].

3 Simulation results and discussion

3.1 Equiaxed dendritic growth

In order to verify the present CA model, a simulation was conducted to simulate the dendritic growth of AZ91 magnesium alloy. A single nucleus was set at the center of the calculation domain which was

divided into 400×400 square cells with a cell size of $1 \mu\text{m}$. No further nucleation was considered then. A uniform temperature field with a cooling rate of 30 K/s was set at the calculation domain. The parameters and physical properties of AZ91 magnesium alloy used in the present simulation are listed in Table 1. Figures 3(a)–(c) show the simulated equiaxed dendritic growth morphology at different simulation times of 0.884, 1.524 and 2.164 s, respectively. According to Fig. 3(a), due to the six-fold symmetry of the crystal lattice, small dendrites appear at the crystallographic orientations with a much faster growing speed than those at the other orientations. As solidification proceeds, the primary arms become larger and the secondary arms branch on the primary arms as shown in Fig. 3(b). With further solidification, the dendrite is well-developed with six-fold symmetry (Fig. 3(c)). Comparing with the micrograph of AZ91 magnesium alloy ingot using polarized light as shown in Fig. 3(d), it is found that the simulated result agrees well with the experimental result relating the dendritic growth morphology.

Using the same parameters mentioned above except for the cooling rate, Fig. 4 indicates the simulated equiaxed dendritic growth of AZ91 magnesium alloy under different cooling rates of 10 and 80 K/s . In conjunction with Fig. 3(c), it can be seen that with an

increase of the cooling rate, the dendrites grow into a more well-developed structure. Only a few secondary arms branch on the primary arms under the cooling rate of 10 K/s (Fig. 4(a)), while the secondary arms develop sufficiently under the cooling rate of 80 K/s , and even some tertiary arms are observed branching on the secondary arms (Fig. 4(b)). Meanwhile, the growth velocity of the dendrites increases with an increase of the cooling rate, which consequently results in a higher accumulation of the solute at the solidification front due to the insufficient solute diffusion.

Table 1 Properties of AZ91 and AM50 magnesium alloys used in present simulations

Property	AZ91	AM50
Initial concentration of Al/%	9.21	5.26
Liquidus temperature/K	868	901
Solidus temperature/K	743	819
Solute partition coefficient	0.4	0.4
Liquidus slope/(K·% ⁻¹)	-6.59	-5.5
Solute diffusion coefficient in liquid/(m ² ·s ⁻¹)	1.8×10^{-9}	1.8×10^{-9}
Solute diffusion coefficient in solid/(m ² ·s ⁻¹)	1.0×10^{-12}	1.0×10^{-12}
Gibbs-Thamson coefficient/(m·K)	6.2×10^{-7}	6.2×10^{-7}

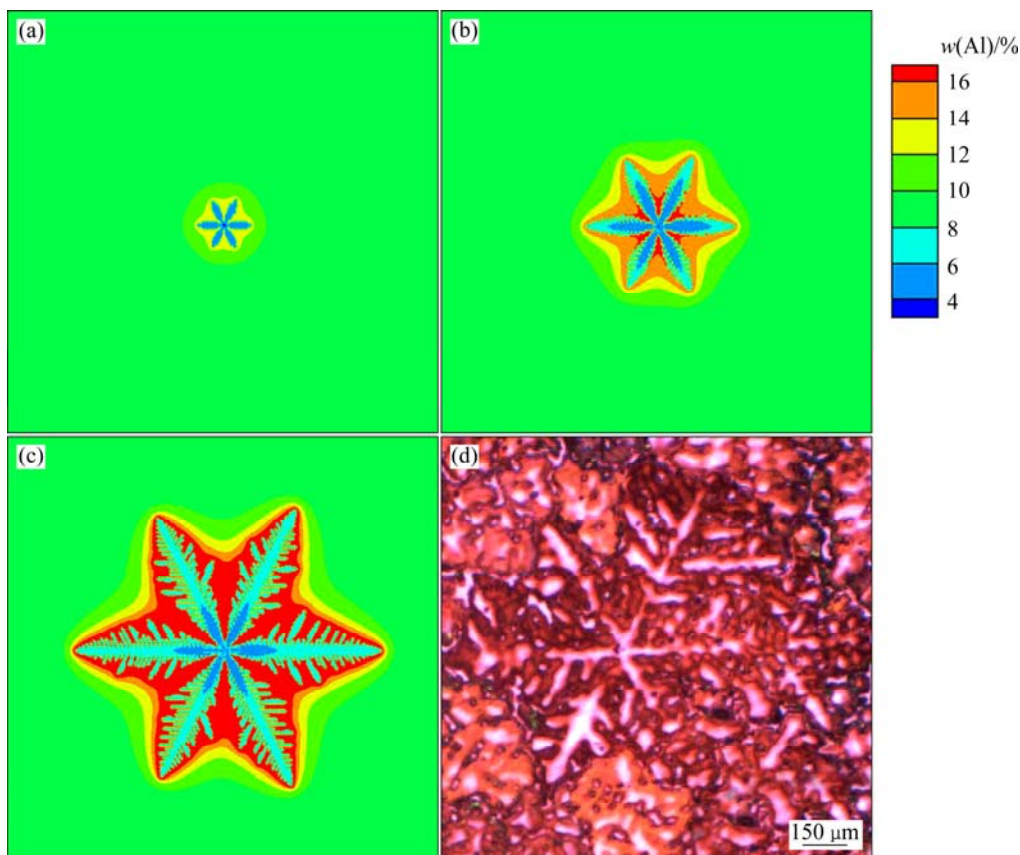


Fig. 3 Simulated (a,b,c) and experimentally observed (d) dendritic morphology with six-fold symmetry: (a) 0.884 s; (b) 1.524 s; (c) 2.164 s; (d) Micrograph of AZ91 magnesium alloy ingot using polarized light

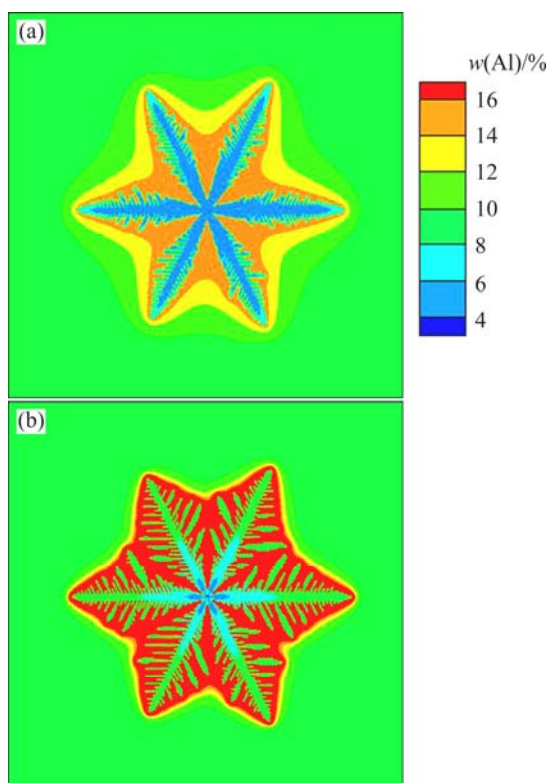


Fig. 4 Simulated equiaxed dendritic growth of AZ91 magnesium alloy under different cooling rates: (a) 10 K/s; (b) 80 K/s

To validate the CA model whether it has the capability to simulate the dendritic growth of magnesium alloy with different growth orientations, a simulation was carried out then. Four nuclei were set at the calculation domain consisting of 500×500 cells with a cell size of $1 \mu\text{m}$. Similarly, no further nucleation was taken into account. Assume that the temperature of the calculation domain is uniform and decreases at a cooling rate of 80 K/s. Figure 5 shows the simulated dendritic growth of AZ91 magnesium alloy with different growth orientations of 0° , 14° , 33.7° and 60° . In the early stages of solidification, the four dendrites generally grow independently with different growth orientations as shown in Fig. 5(a). As solidification proceeds, the growth of the dendrites is gradually influenced by each other with the solute field as the medium (Fig. 5(b)). It can be seen from Fig. 5(c) that the dendrites impinge on each other, which results in coarsening of the dendrites. Meanwhile, tertiary branches develop almost only on the side of the secondary branches facing the primary dendrite tips. The solute accumulates in the liquid ahead of the dendrite tips and also in the interdendritic liquid, which may result in the eutectic formation at the grain boundary of the primary α -Mg. However, the formation of the eutectics was not taken into account in the present work.

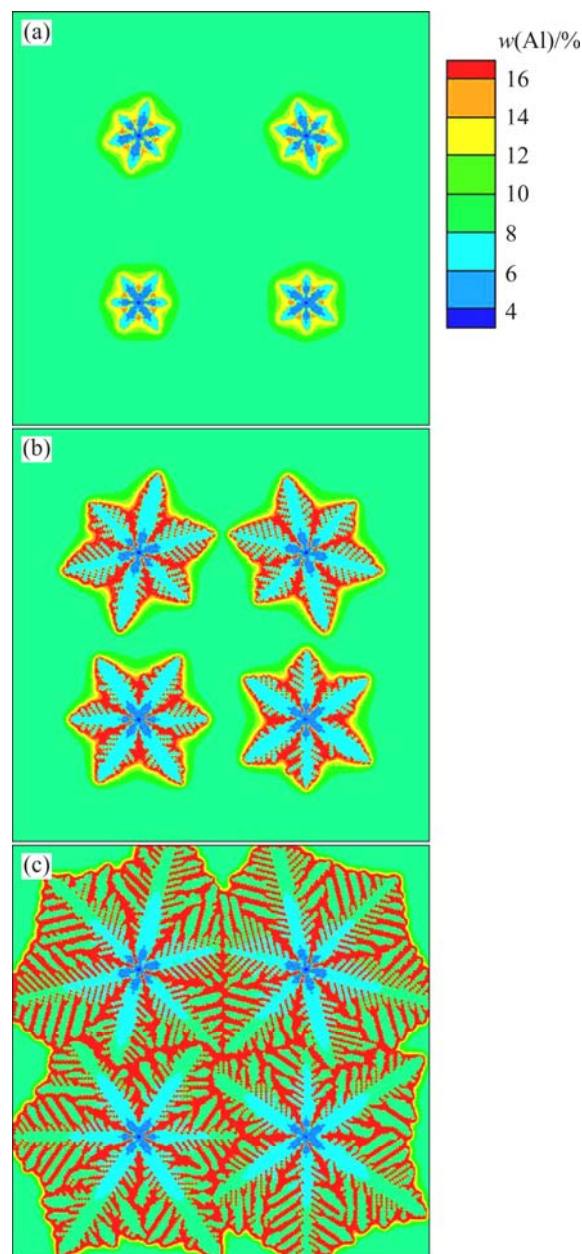


Fig. 5 Simulated dendritic growth of AZ91 magnesium alloy with different growth orientations of 0° , 14° , 33.7° and 60° : (a) 0.584 s; (b) 0.984 s; (c) 1.184 s

3.2 Columnar dendritic growth

The present model was applied to simulate the columnar dendritic growth of AM50 magnesium alloy under directional solidification. As it is known that the dendritic growth under directional solidification is mainly affected by the solidification rate (v) and the temperature gradient (G_L), in the case study, the effect of the two parameters on the dendritic growth morphology was investigated. Ten nuclei were set at the bottom of the calculation domain consisting of 200×500 cells with a uniform interval. The cell size was $4 \mu\text{m}$. A positive temperature gradient of G_L was set along the y direction of the calculation domain, while the initial temperature

of the cells at the bottom was arranged to be equal to the liquidus temperature. As the calculation proceeded, the temperature of the whole calculation domain decreased at a cooling rate of R_C . In this case, the solidification rate under directional solidification was: $v=R_C/G_L$. The parameters and physical properties of AM50 magnesium alloy used in the case study are also listed in Table 1. Figure 6 indicates the columnar dendritic growth of AM50 magnesium alloy under directional solidification at different solidification rates and temperature gradients. It can be seen that the primary arms grow along the direction of the temperature gradient. Secondary arms branch on the primary arms and still form an angle of 60° with respect to the primary arms (Figs. 6(a) and (b)). However, the growth of the secondary arms is retarded in Fig. 6(c) as there is only a little small space for their development.

Meanwhile, it can be illustrated from Figs. 6(a) and

(b) that with the same temperature gradient, more dendrites form and grow from the nuclei at the bottom of the calculation domain with an increase of the solidification rate. According to Figs. 6(b) and (c), the same trend is also found by increasing the temperature gradient, while the solidification rate keeps unchanged. In other words, the primary arm spacing (λ_1) decreases with an increase of both the solidification rate (v) and the temperature gradient (G_L). The simulated results are in accordance with the analytical model ($\lambda_1 \propto G_L^{-0.5} v^{-0.25}$) proposed by HUNT et al [18].

Figure 7 shows the simulated dendritic growth of AM50 magnesium alloy under directional solidification with a temperature gradient of 27 K/mm and a cooling rate of 2.5 K/s. The direction of the temperature gradient forms an angle of 60° with respect to the x coordinate. It can be found that since the dendrites grow along the direction of the temperature gradient, the growth of the

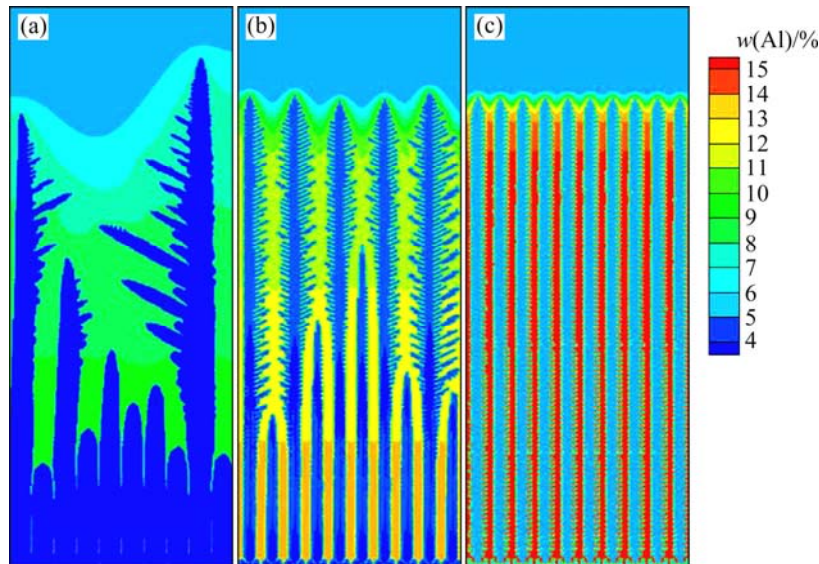


Fig. 6 Simulated columnar dendritic growth of AM50 magnesium alloy under directional solidification at different solidification rates and temperature gradients: (a) $G_L=10$ K/mm, $v=2.5 \times 10^{-5}$ m/s; (b) $G_L=10$ K/mm, $v=2.5 \times 10^{-4}$ m/s; (c) $G_L=50$ K/mm, $v=2.5 \times 10^{-4}$ m/s

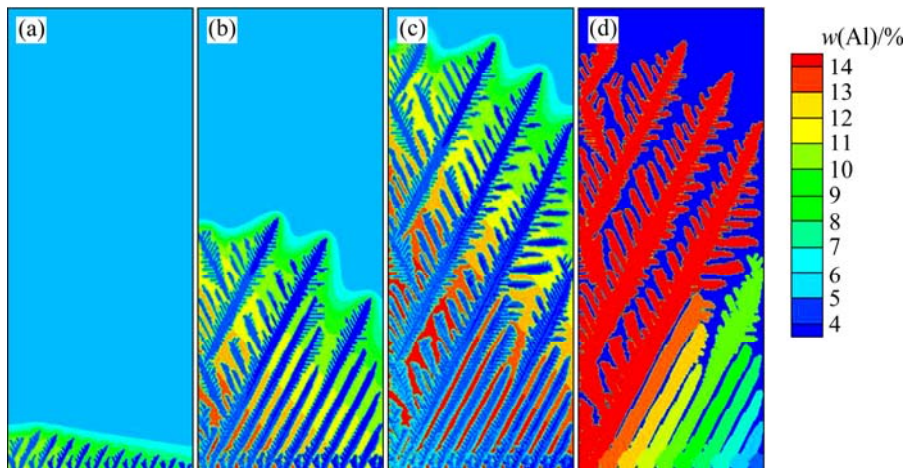


Fig. 7 Simulated dendritic growth of AM50 magnesium alloy under directional solidification when direction of temperature gradient forms an angle of 60° with respect to x coordinate: (a) 1.764 s; (b) 9.444 s; (c) 15.844 s; (d) Grains displayed with different colors

dendrites on the right hand side is retarded, while the leftmost dendrite is well-developed with branching of secondary, tertiary and even higher order dendrite arms.

In order to investigate the competitive growth mechanism of dendrites with different growth orientations, a simulation was further conducted. The calculation domain consists of 400×600 cells with a cell size of $4 \mu\text{m}$. Five nuclei with different initial orientations were set at the bottom of the calculation domain. With a cooling rate of 2.5 K/s and a temperature gradient of 20 K/mm along the y direction of the calculation domain, Fig. 8 indicates the dendritic growth of AM50 magnesium alloy with different growth orientations the same as in Fig. 5. It can be seen that as the solidification proceeds, the dendrites with their growth orientations aligned with the direction of temperature gradient grow faster than the other dendrites. Finally, the growth of the second and third dendrites on the left is blocked. Meanwhile, some tertiary arms of the first and last dendrites are well-developed and grow parallel to their primary arms and also the direction of the temperature gradient.

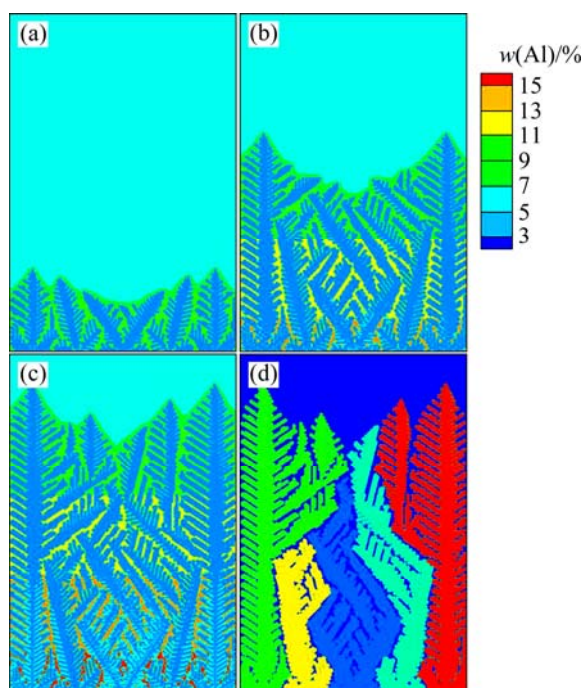


Fig. 8 Competitive growth of dendrites of AM50 magnesium alloy under directional solidification with different growth orientations: (a) 3.044 s; (b) 9.444 s; (c) 14.244 s; (d) Grains displayed with different colors

4 Conclusions

A two-dimensional cellular automaton model was developed to simulate the dendritic growth of magnesium alloy. By defining a special neighborhood configuration with the square CA cell and applying a set

of capturing rules, modeling of dendritic growth of magnesium alloy with six-fold symmetry and different growth orientation was achieved. During simulation of the equiaxed dendritic growth, it can be found that the dendrites grow into a more well-developed structure with an increase of the cooling rate. Under directional solidification process, the dendrites with their growth orientations aligned with the direction of the temperature gradient grow faster than the other dendrites. Meanwhile, the primary arm spacing decreases with an increase of both the solidification rate and the temperature gradient. The simulated results are consistent with the experimental results and the analytical model.

References

- [1] FRIEDRICH H, SCHUMANN S. Research for a “new age of magnesium” in the automotive industry [J]. *Journal of Materials Processing Technology*, 2001, 117: 276–281.
- [2] CHEN Dong-feng, DONG Xuan-pu, ZHANG Xiong, FAN Zi-tian. Mg alloy surface alloying layer fabricated through evaporative pattern casting technology [J]. *Transaction of Nonferrous Metals Society of China*, 2010, 20: 2240–2245.
- [3] AGHION E, BRONFIN B, ELIEZER D. The role of the magnesium industry in protecting the environment [J]. *Journal of Materials Processing Technology*, 2001, 117: 381–385.
- [4] ZHU Ming-fang, PAN Shi-yan, SUN Dong-ke, ZHAO Hong-lei. Numerical simulation of microstructure evolution during alloy solidification by using cellular automaton method [J]. *ISIJ International*, 2010, 50(12): 1851–1858.
- [5] WANG W, LEE P D, McLEAN M. A model of solidification microstructures in nickel-based superalloys: Predicting primary dendrite spacing selection [J]. *Acta Materialia*, 2003, 51: 2971–2987.
- [6] BELTRAN-SANCHEZ L, STEFANESCU D M. Growth of solutal dendrites: A cellular automaton model and its quantitative capabilities [J]. *Metallurgical and Materials Transactions A*, 2003, 34: 367–382.
- [7] SHAN Bo-wei, HUANG Wei-dong, LIN Xin, WEI Lei. Dendrite primary spacing selection simulation by the cellular automaton model [J]. *Acta Metallurgica Sinica*, 2008, 44(9): 1042–1050. (in Chinese)
- [8] KANG Xiu-hong, DU Qiang, LI Dian-zhong, LI Yi-yi. Modeling of the solidification microstructure evolution by coupling cellular automaton with macro-transport model [J]. *Acta Metallurgica Sinica*, 2004, 40(5): 452–456. (in Chinese)
- [9] HUO L, HAN Z Q, LIU B C. Three-dimensional modeling and simulation of dendrite morphology of cast Mg alloys [J]. *Materials Science Forum*, 2010, 654–656: 1516–1519.
- [10] YIN H B, FELICELLI S D. A cellular automaton model for dendrite growth in magnesium alloy AZ91 [J]. *Modelling and Simulation in Materials Science and Engineering*, 2009, 17: 075011-1–075011-15.
- [11] FU Zhen-nan, XU Qing-yan, XIONG Shou-mei. Numerical simulation on dendrite growth process of Mg alloy using cellular automaton method based on probability capturing model [J]. *The Chinese Journal of Nonferrous Metals*, 2007, 17(10): 1567–1573. (in Chinese)
- [12] SASIKUMAR R, SREENIVASAN R. Two dimensional simulation of dendrite morphology [J]. *Acta Metallurgica et Materialia*, 1994, 42(7): 2381–2386.
- [13] GANDIN C A, RAPPAZ M. A coupled finite element-cellular automaton model for the prediction of dendritic grain structures in

- solidification process [J]. *Acta Metallurgica et Materialia*, 1994, 42(7): 2233–2246.
- [14] BELTRAN-SANCHEZ L, STEFANESCU D M. A quantitative dendrite growth model and analysis of stability concepts [J]. *Metallurgical and Materials Transactions A*, 2004, 35: 2471–2485.
- [15] ZHU M F, STEFANESCU D M. Virtual front tracking model for the quantitative modeling of dendritic growth in solidification alloys [J]. *Acta Materialia*, 2007, 55: 1741–1755.
- [16] BELTRAN-SANCHEZ L, STEFANESCU D M. Growth of solutal dendrites—A cellular automaton model [J]. *International Journal of Cast Metals Research*, 2002, 15: 251–256.
- [17] WU Meng-wu, XIONG Shou-mei. Microstructure simulation of high pressure die cast magnesium alloy based on modified CA method [J]. *Acta Metallurgica Sinica*, 2010, 46(12): 1534–1542. (in Chinese)
- [18] HUNT J D, LU S Z. Numerical modeling of cellular/dendritic array growth: Spacing and structure predictions [J]. *Metallurgical and Materials Transactions A*, 1996, 27: 611–623.

镁合金等轴及柱状树枝晶模拟

吴孟武^{1,2}, 熊守美^{1,2}

1. 清华大学 机械工程系, 北京 100084;
2. 清华大学 汽车安全与节能国家重点实验室, 北京 100084

摘要: 基于CA方法, 开发了模拟具有HCP晶体结构的镁合金的枝晶生长模型, 生长动力学通过求解传输方程获得。通过定义特殊的正方网格CA邻居单元及采用由BELTRAN-SANCHEZ 和 STEFANESCU提出的具有立方晶体结构的金属凝固过程中枝晶生长的捕获规则, 实现了具有不同生长取向的镁合金枝晶生长的建模及仿真。对镁合金等轴树枝晶和定向凝固条件下柱状树枝晶的生长进行模拟。对模拟结果与实验结果及发表的实验结果进行对比, 从而验证了模型的可靠性。

关键词: 镁合金; 枝晶生长; CA方法; 生长取向

(Edited by YUAN Sai-qian)